Investigation of Backgate-Bias Dependence of Threshold-Voltage Sensitivity to Process and Temperature Variations for Ultra-Thin-Body Hetero-Channel MOSFETs

Chang-Hung Yu, *Student Member, IEEE*, and Pin Su, *Member, IEEE*

***Abstract*—This paper investigates the impact of backgate bias ($\mathrm{V_{bg}}$) on the sensitivity of threshold voltage ($\mathrm{V_{th}}$) to process and temperature variations for ultra-thin-body (UTB) GeOI and InGaAs-OI MOSFETs. Our study indicates that the quantum-confinement effect significantly suppresses the $\mathrm{V_{bg}}$ dependence of the $\mathrm{V_{th}}$ sensitivity to process and temperature variations. Since Si, Ge, and InGaAs channels exhibit different degrees of quantum confinement, the impact of quantum confinement has to be considered when one-to-one comparisons among hetero-channel UTB devices regarding variability are made. Our study is crucial to the robustness of multi-$\mathrm{V_{th}}$ designs with advanced UTB technologies.**

***Index Terms*—Backgate bias, germanium-on-insulator (GeOI), InGaAs-OI, process variation, quantum confinement (QC), temperature variation, ultra-thin-body (UTB).**

I. Introduction

VARIABILITY of nanoscale MOSFETs has become a crucial concern to the functional robustness of integrated circuits and systems [1]–[5]. For future CMOS devices, Ge and III–V materials such as InGaAs have been proposed as alternative channel material because of their superior transport properties [6]–[10]. Their higher permittivity, however, makes them more susceptible to short-channel effects (SCEs). Ultra-thin-body (UTB) structure with thin buried oxide (BOX) has been regarded as one of the promising solutions to improve the electrostatic integrity (EI) [9]–[12]. In addition to its immunity to SCEs and reduced random dopant fluctuation (RDF) by employing undoped (or lightly doped) channel [13]–[15], using the UTB with thin BOX structure also enables more efficient threshold voltage ($\mathrm{V_{th}}$) modulation through backgate bias ($\mathrm{V_{bg}}$) for power/performance optimization [11], [12] and global variability compensation [16]–[19]. With the scaling of device dimensions, the quantum-confinement (QC) effect along the channel-thickness direction may become significant.

Manuscript received November 9, 2012; revised April 20, 2013; accepted April 23, 2013. Date of publication May 7, 2013; date of current version March 4, 2014. This work was supported in part by the National Science Council of Taiwan under contracts NSC 102-2221-E-009-136-MY2 and NSC 102-2911-I-009-302 (I-RiCE), and in part by the Ministry of Education in Taiwan under ATU program. *(Corresponding author: P. Su.)*

The authors are with the Department of Electronics Engineering and the Institute of Electronics, National Chiao Tung University, Hsinchu 30010, Taiwan (e-mail: pinsu@faculty.nctu.edu.tw).

Color versions of one or more of the figures in this paper are available online at http://ieeexplore.ieee.org.

Digital Object Identifier 10.1109/TDMR.2013.2262115

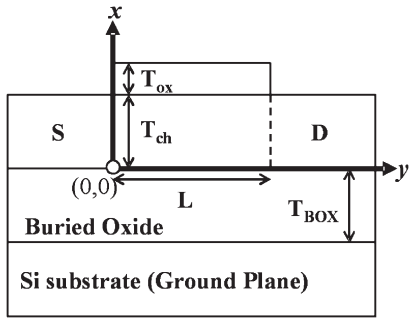

Fig. 1. Schematic sketch of a UTB structure with thin buried oxide (BOX). The origin point is located at the channel/BOX interface of source/channel junction. L is the channel length. $\mathrm{T_{ch}}$, $\mathrm{T_{ox}}$ and $\mathrm{T_{BOX}}$ are thicknesses of channel, gate oxide and BOX, respectively. The doping concentration of the Si ground plane is 1×10^{20} $\mathrm{cm^{-3}}$ (p-type).

Whether the QC effect will impact the $\mathrm{V_{bg}}$ dependence of the $\mathrm{V_{th}}$ variability for these UTB hetero-channel devices has rarely been discussed and merits detailed investigation.

In this paper, using an analytical solution of Schrödinger equation corroborated with TCAD simulation, we investigate the impact of backgate bias on the sensitivity of $\mathrm{V_{th}}$ to channel length (L), channel thickness ($\mathrm{T_{ch}}$), and temperature (T) variations for UTB GeOI and InGaAs-OI n-MOSFETs. This paper is organized as follows. In Section II, we describe our model for UTB MOSFETs used in the work. In Section III, we investigate and compare the impact of backgate bias on the sensitivity of $\mathrm{V_{th}}$ to process variations for GeOI and InGaAs-OI devices. The implication on within-die variability is also discussed. Examination of the $\mathrm{V_{bg}}$ dependence of the $\mathrm{V_{th}}$ sensitivity to temperature variation is presented in Section IV. The conclusion is drawn in Section V.

II. Methodology

Fig. 1 shows a schematic sketch of a UTB with thin BOX structure. To consider the quantum-confinement effect along the channel-thickness (i.e., x) direction, the 1-D Schrödinger equation needs to be solved. In order to obtain an analytical quantum-confinement model, the conduction-band edge $E_C(x)$ was usually treated as a triangular well [20]. To consider the SCEs in this work, however, it is treated as a parabolic well [21] with $E_C(x) = \alpha x^2 + \beta x + \gamma$, where α, β, and γ are channel-length-dependent coefficients and can be obtained

from the channel potential solution of Poisson's equation under subthreshold region [22]. Utilizing the parabolic-well treatment and the power series method, the wave function can be expressed as $\Psi_j = \Sigma d_n \cdot x^n$ with [21]

$$d_2 = -\frac{m_x}{\hbar^2}(E_j - \gamma) \cdot d_0;$$
$$d_3 = -\frac{m_x}{3\hbar^2}\left[(E_j - \gamma) \cdot d_1 - \beta \cdot d_0\right]$$
$$d_n = -\frac{2m_x}{n(n-1)\hbar^2}\left[(E_j - \gamma) \cdot d_{n-2} - \beta \cdot d_{n-3} - \alpha \cdot d_{n-4}\right], \quad n \geq 4 \qquad (1)$$

where E_j is the jth eigenenergy and m_x is the carrier quantization effective mass [23].

The eigenenergies and wave functions of short-channel UTB MOSFETs under subthreshold region can then be derived by the boundary condition $\Psi_j(x = 0) = \Psi_j(x = \mathrm{T_{ch}}) = 0$ with $x = 0$ and $x = \mathrm{T_{ch}}$ defined as the interfaces of BOX/channel and channel/gate-oxide, respectively. Utilizing the derived eigenenergies and wave functions, the channel electron density can be calculated by [23]

$$n(x, y) = N_{C,\mathrm{QM}}(x, y) \cdot \exp\left(\frac{E_F(y) - E_C(x, y)}{kT}\right) \qquad (2a)$$

$$N_{C,\mathrm{QM}}(x, y) = \sum_{\nu,j}\left\{\frac{g_\nu m_{d,\nu} kT}{\pi\hbar^2} \cdot \exp\left(\frac{E_C(x, y) - E_{j,\nu}}{kT}\right) \cdot |\Psi_{j,\nu}(x, y)|^2\right\} \qquad (2b)$$

where ν is the type of valley, g_ν is the degeneracy of the valley, $m_{d,\nu}$ is the corresponding density-of-state effective mass [23], [24], and $E_F(y)$ is the quasi-Fermi level along the channel-length (i.e., y) direction. It should be noted that the impact of quantized eigenenergies and wave functions on the electron density is incorporated into the effective density-of-state for conduction band $(N_{C,\mathrm{QM}})$ [25] and the subthreshold drain current in terms of $N_{C,\mathrm{QM}}$ can be obtained [21], [26], [27].

Our quantum-confinement model has been verified with TCAD simulation that numerically solves the self-consistent solution of 2-D Poisson and 1-D Schrödinger equation [28]. In this study, the source/drain doping concentration is 5.5×10^{19} cm^{-3} for the GeOI device and 1×10^{20} cm^{-3} for the InGaAs-OI device. Abrupt junction between the source/drain region and the channel region is assumed. The transport model we employed is the drift-diffusion model with constant mobility (3,900 cm^2/V $\cdot$ s for Ge and 15,000 cm^2/V $\cdot$ s for InGaAs [32], [33]). Fig. 2(a) and (b) show that for both the parabolic potential well of short-channel devices and the triangular well of long-channel devices with forward and reverse $\mathrm{V_{bg}}$, the E_j's can be accurately predicted by our QC model. It is worth noting from Fig. 2(b) that, the triangular potential well of $\mathrm{V_{bg}} = -1$ V is much sharper than that of $\mathrm{V_{bg}} = 1$ V, and thus the eigenenergies of $\mathrm{V_{bg}} = -1$ V are higher than the $\mathrm{V_{bg}} = 1$ V counterparts. Fig. 3(a) and (b) show that our calculated subthreshold drain current considering the QC effect

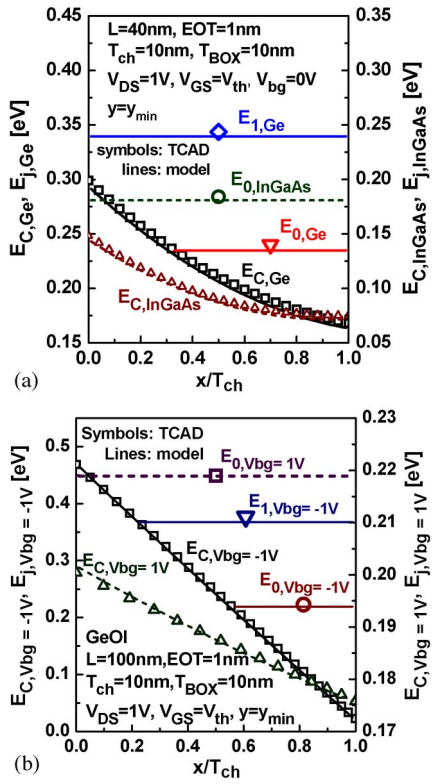

Fig. 2. Conduction-band edge E_C and quantized eigenenergies of UTB MOSFETs. (a) Short-channel GeOI and InGaAs-OI devices with parabolic well at $\mathrm{V_{bg}} = 0$ V. (b) Long-channel GeOI device with triangular well for $\mathrm{V_{bg}} = -1$ V and $\mathrm{V_{bg}} = 1$ V. $\mathrm{y_{min}}$ is where the minimum potential occurs for carrier flow along the channel-length direction.

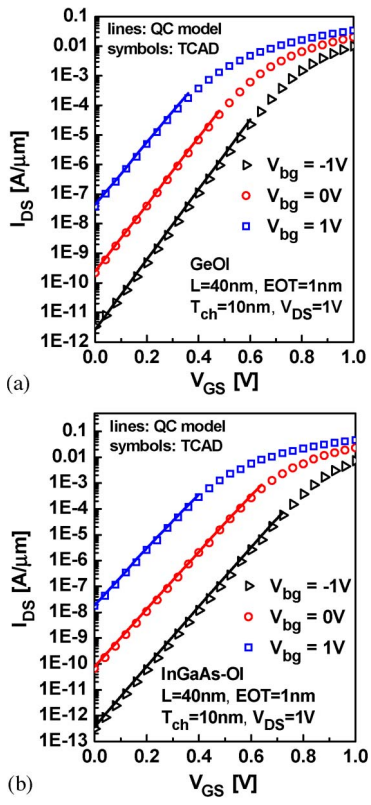

Fig. 3. Verification of the $\log(\mathrm{I_{DS}})$ vs. $\mathrm{V_{GS}}$ characteristics of (a) UTB GeOI, and (b) InGaAs-OI devices for our quantum-confinement model.

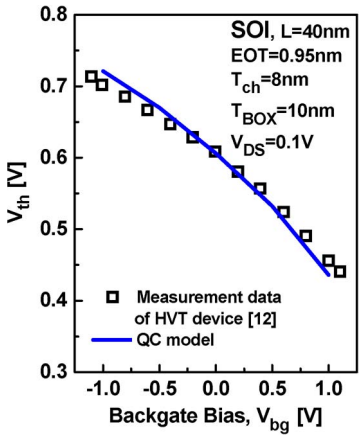

Fig. 4. Comparison of the sensitivity of V_{th} to V_{bg} for our quantum-confinement model and the experimental data from [12].

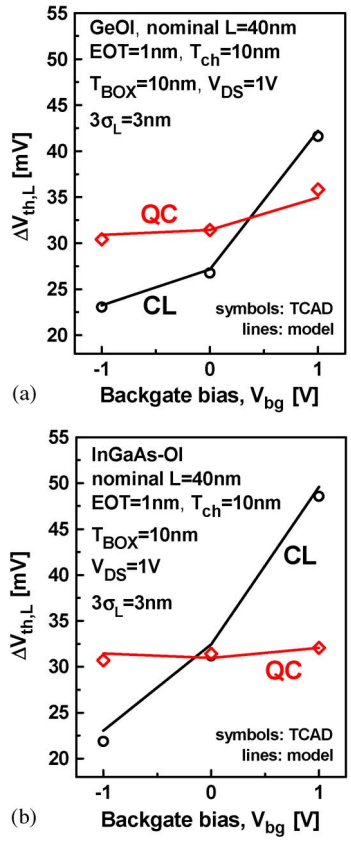

Fig. 5. Impact of quantum confinement on the sensitivity of $\Delta V_{th,L}$ to V_{bg} for (a) UTB GeOI, and (b) InGaAs-OI devices with nominal $L = 40$ nm. $\Delta V_{th,L}$ denotes the V_{th} variation caused by the L variation. CL: classical condition. Noted that $V_{th} = V_{gs}$ (when $I_{ds} = 100$ nA $\times$ (W/L)).

is fairly accurate as compared with the TCAD simulation. Fig. 4 shows that the sensitivity of V_{th} to V_{bg} exhibits satisfactory agreement between the model and the experimental data [12].

III. Impact of Backgate Bias on Threshold-Voltage Sensitivity to Process Variations

In this work, we use $\Delta V_{th} = |V_{th}(+3\sigma) - V_{th}(-3\sigma)|/2$ to represent the sensitivity of V_{th} to process variations. Based on [31], the standard deviations of L variation (σ_L) and T_{ch} variation (σ_{Tch}) are assumed to be 1 nm and 0.16 nm, respectively, in our calculation [31]. The V_{th} is determined by adopting a constant current criteria of 100 nA $\times$ (W/L). Fig. 5 compares the impact of quantum confinement on the backgate-bias dependence of V_{th} sensitivity to L variation for GeOI and InGaAs-OI devices with nominal $L = 40$ nm. It can be seen that, for both the GeOI and InGaAs-OI devices, the L-induced V_{th} variation ($\Delta V_{th,L}$) increases significantly with increasing V_{bg} (i.e., from reverse to forward backgate bias) under the classical (CL) condition. This is because the carrier centroid is moved toward the backgate interface from reverse to forward V_{bg}. However, as the QC effect is considered, the sensitivity $\Delta V_{th,L}$ is less dependent on V_{bg} for both the GeOI and InGaAs-OI devices. In addition, Fig. 5 also shows that the worst-case $\Delta V_{th,L}$ is reduced by the QC effect at $V_{bg} = 1$ V. Fig. 6(a) shows that, as compared with the CL condition, the V_{th} roll-off is deteriorated by the QC effect for GeOI devices with $V_{bg} = -1$ V so that the $\Delta V_{th,L}$ considering the QC effect is higher than the CL counterpart. In Fig. 6(b) with $V_{bg} = 1$ V, on the contrary, the V_{th} roll-off is suppressed by the QC effect and hence the $\Delta V_{th,L}$ considering the QC effect is lower than the CL one. This explains the QC-reduced V_{bg}-dependence of $\Delta V_{th,L}$ in Fig. 5. The opposite trend of V_{th} roll-off for the GeOI device with $V_{bg} = -1$ V and $V_{bg} = 1$ V can be explained by Fig. 7, where the ground-state eigenenergy ($E_0 - E_{C,\min}$) (and thus the QC-induced V_{th} shift) of the long-channel GeOI device ($L = 100$ nm) is essentially much higher than the short-channel

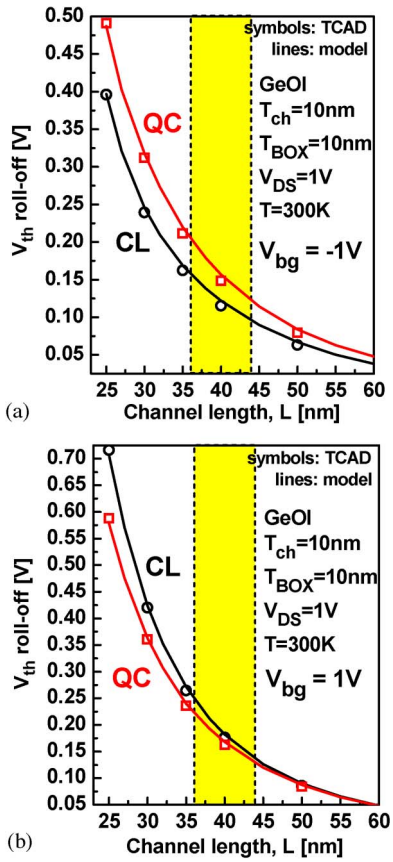

Fig. 6. Impact of quantum confinement on the V_{th} roll-off for UTB GeOI devices with (a) $V_{bg} = -1$ V, and (b) $V_{bg} = 1$ V. The V_{th} roll-off is defined as $V_{th}(L = 100\text{ nm}) - V_{th}(L)$.

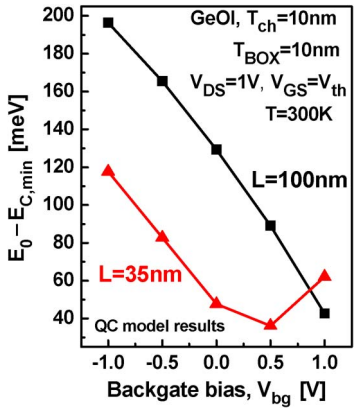

Fig. 7. Impact of $\mathrm{V_{bg}}$ on the ground-state eigenenergy $(E_0 - E_{C,\min})$ of long-channel and short-channel UTB GeOI devices with $\mathrm{T_{ch}} = 10$ nm.

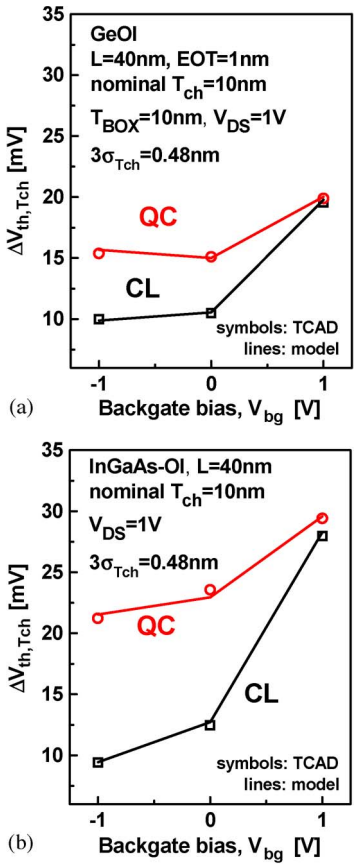

Fig. 8. Impact of quantum confinement on the sensitivity of $\Delta \mathrm{V_{th,Tch}}$ to $\mathrm{V_{bg}}$ for (a) UTB GeOI, and (b) InGaAs-OI devices with $\mathrm{L} = 40$ nm. $\Delta \mathrm{V_{th,Tch}}$ denotes the $\mathrm{V_{th}}$ variation caused by the $\mathrm{T_{ch}}$ variation.

one at $\mathrm{V_{bg}} = -1$ V because of the sharp triangular well. The $(E_0 - E_{C,\min})$ as well as the QC-induced $\mathrm{V_{th}}$ shift of the long-channel device substantially decreases with increasing $\mathrm{V_{bg}}$ due to the strong $\mathrm{V_{bg}}$ modulation of its triangular well [Fig. 2(b)]. Therefore, the $\mathrm{V_{th}}$ roll-off is deteriorated by the QC effect for the GeOI device at $\mathrm{V_{bg}} = -1$ V, while it shows the opposite trend at $\mathrm{V_{bg}} = 1$ V in Fig. 6.

It is worth noting from Fig. 5 that if Adaptive Body Bias (ABB) is used to compensate the systematic die-to-die variation, the corrective application of $\mathrm{V_{bg}}$ (positive or negative) on a given die would significantly vary the within-die $\mathrm{V_{th}}$

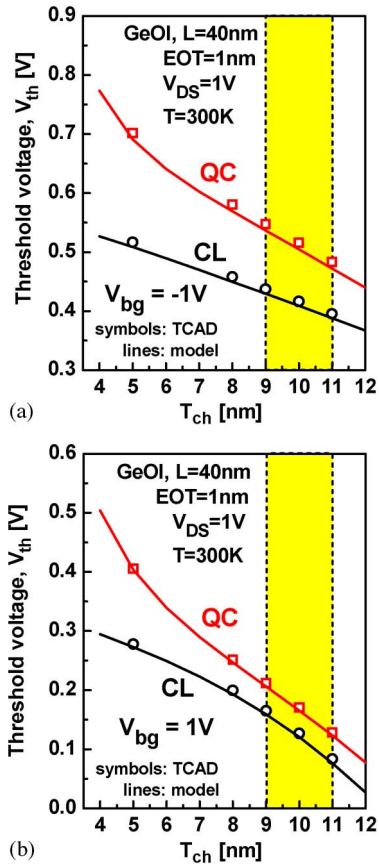

Fig. 9. Impact of quantum confinement on the sensitivity of $\mathrm{V_{th}}$ to $\mathrm{T_{ch}}$ for UTB GeOI devices with (a) $\mathrm{V_{bg}} = -1$ V, and (b) $\mathrm{V_{bg}} = 1$ V.

variability according to the CL model. However, this effect can be beneficially suppressed by the QC effect.

Fig. 8 compares the impact of backgate bias on the sensitivity of $\mathrm{V_{th}}$ to $\mathrm{T_{ch}}$ variation under the QC and CL conditions for GeOI and InGaAs-OI devices with nominal $\mathrm{T_{ch}} = 10$ nm. It can be seen that the $\Delta \mathrm{V_{th}}$ caused by the $\mathrm{T_{ch}}$ variation $(\Delta \mathrm{V_{th,Tch}})$ increases with $\mathrm{V_{bg}}$ under the CL condition for both the GeOI and InGaAs-OI devices because the device electrostatic integrity deteriorates as $\mathrm{V_{bg}}$ increases. Moreover, both the GeOI and InGaAs-OI devices exhibit less $\mathrm{V_{bg}}$-dependence of $\Delta \mathrm{V_{th,Tch}}$ as the QC effect is considered, although for a given $\mathrm{V_{bg}}$ (e.g., $\mathrm{V_{bg}} = -1$ V) the magnitude of $\Delta \mathrm{V_{th,Tch}}$ is increased by the QC effect. It is also worth noting that the worst-case $\Delta \mathrm{V_{th,Tch}}$ occurring at $\mathrm{V_{bg}} = 1$ V is hardly changed by the QC effect. Fig. 9(a) indicates that the QC-induced $\mathrm{V_{th}}$ shift of the GeOI devices with $\mathrm{V_{bg}} = -1$ V decreases with increasing $\mathrm{T_{ch}}$. In Fig. 9(b) with $\mathrm{V_{bg}} = 1$ V, the QC-induced $\mathrm{V_{th}}$ shift, however, becomes comparable around $\mathrm{T_{ch}} = 10$ nm. In other words, at $\mathrm{V_{bg}} = -1$ V, the $\Delta \mathrm{V_{th,Tch}}$ considering the QC effect is higher than the CL counterpart, while it becomes comparable to the CL at $\mathrm{V_{bg}} = 1$ V. Fig. 10 shows that the $(E_0 - E_{C,\min})$ (and thus the QC-induced $\mathrm{V_{th}}$ shift) of $\mathrm{V_{bg}} = -1$ V decreases with increasing $\mathrm{T_{ch}}$, while the $(E_0 - E_{C,\min})$ of $\mathrm{V_{bg}} = 1$ V saturates at around $\mathrm{T_{ch}} = 8$ nm. It is plausible that the degree of electrical confinement decreases as $\mathrm{V_{bg}}$ increases, so the $\mathrm{V_{bg}}$ dependence of $\Delta \mathrm{V_{th,Tch}}$ is suppressed by the QC effect for both the GeOI and InGaAs-OI devices in Fig. 8.

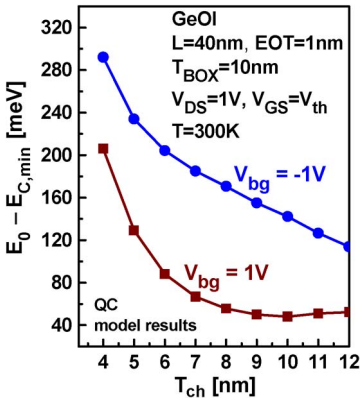

Fig. 10. Difference of ground-state eigenenergy $(E_0 - E_{C,\min})$ between $\mathrm{V_{bg}} = -1$ V and $\mathrm{V_{bg}} = 1$ V for UTB GeOI devices with various $\mathrm{T_{ch}}$.

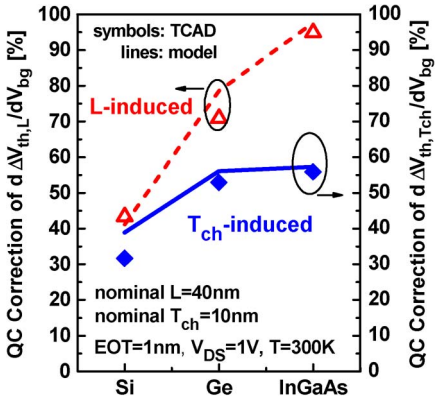

Fig. 11. Comparison of the impact of quantum confinement on the sensitivity of L-induced and $\mathrm{T_{ch}}$-induced $\mathrm{V_{th}}$ variations to $\mathrm{V_{bg}}$ for UTB SOI, GeOI, and InGaAs-OI devices.

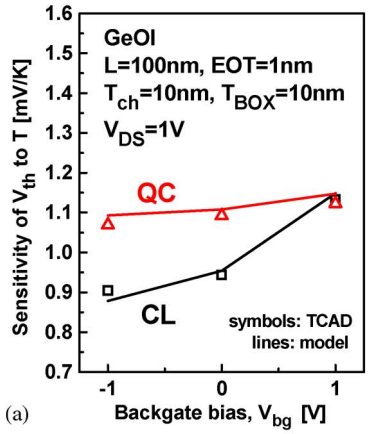

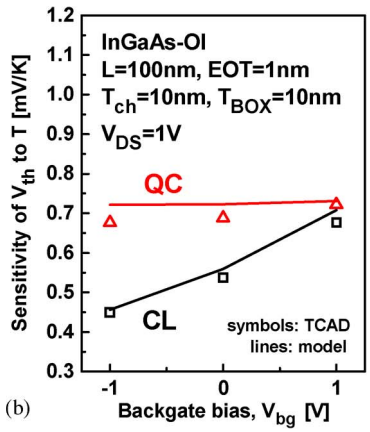

Fig. 12. Impact of quantum confinement on the $\mathrm{V_{bg}}$ dependence of the $\mathrm{V_{th}}$ sensitivity to temperature for (a) UTB GeOI, and (b) InGaAs-OI devices. The sensitivity of $\mathrm{V_{th}}$ to temperature $(|\Delta \mathrm{V_{th}}/\Delta \mathrm{T}|)$ is defined as $|\mathrm{V_{th}}(\mathrm{T} = 400\ \mathrm{K}) - \mathrm{V_{th}}(\mathrm{T} = 200\ \mathrm{K})|/(400\ \mathrm{K} - 200\ \mathrm{K})$.

Fig. 11 compares the impact of quantum confinement on the sensitivity of process-induced $\mathrm{V_{th}}$ variations to $\mathrm{V_{bg}}$ for Si-, Ge- and InGaAs-channel devices. Here, the $\mathrm{d}\Delta \mathrm{V_{th}}/\mathrm{dV_{bg}}$ denotes $\Delta \mathrm{V_{th}}(\mathrm{V_{bg}} = 1\ \mathrm{V}) - \Delta \mathrm{V_{th}}(\mathrm{V_{bg}} = -1\ \mathrm{V})$ and the QC correction means the percentage change of $\mathrm{d}\Delta \mathrm{V_{th}}/\mathrm{dV_{bg}}$ due to quantum confinement. It can be seen that the QC effect suppressing the $\mathrm{V_{bg}}$-dependence of the $\mathrm{V_{th}}$ sensitivity to L and $\mathrm{T_{ch}}$ variations applies to standard Si devices in addition to high-mobility channel devices. However, due to the difference in the quantization effective mass, the InGaAs-channel device exhibits the largest QC correction, whereas the Si device exhibits the smallest QC correction.

IV. Impact of Backgate Bias on Threshold-Voltage Sensitivity to Temperature Variation

Fig. 12 compares the impact of quantum confinement on the backgate-bias dependence of the $\mathrm{V_{th}}$ sensitivity to temperature for UTB GeOI and InGaAs-OI devices. It shows that the sensitivity of $\mathrm{V_{th}}$ to temperature $(|\Delta \mathrm{V_{th}}/\Delta \mathrm{T}|)$ increases with $\mathrm{V_{bg}}$ under the CL condition for both GeOI and InGaAs-OI devices. It can also be seen that, for a given $\mathrm{V_{bg}}$ (e.g. $\mathrm{V_{bg}} = -1$ V), the $|\Delta \mathrm{V_{th}}/\Delta \mathrm{T}|$ is increased by the QC effect. Moreover, the QC-increased $|\Delta \mathrm{V_{th}}/\Delta \mathrm{T}|$ of the InGaAs-OI device is larger than the GeOI counterpart. The $\mathrm{V_{bg}}$-dependence of $|\Delta \mathrm{V_{th}}/\Delta \mathrm{T}|$, however, is reduced considering the QC effect. Fig. 12 also indicates that the worst-case $|\Delta \mathrm{V_{th}}/\Delta \mathrm{T}|$ under $\mathrm{V_{bg}} = 1$ V is nearly unchanged after considering the QC effect. Fig. 13(a) shows that the QC-induced $\mathrm{V_{th}}$ shift at $\mathrm{T} = 200$ K is larger than that at $\mathrm{T} = 400$ K for $\mathrm{V_{bg}} = -1$ V, while they are comparable for $\mathrm{V_{bg}} = 1$ V. This can be explained as follows. The QC-induced $\mathrm{V_{th}}$ shift, $\Delta V_{\mathrm{th}}^{\mathrm{QM}}$, is mainly determined by the equivalent surface potential shift $\Delta \psi_s^{\mathrm{QM}}$ [29], which depends on the ground-state eigenenergy $(E_0 - E_{C,\min})$ and the location of carrier centroid under the ground-state approximation [20], [29], [30]. Fig. 13(b) shows that the $(E_0 - E_{C,\min})$ at $\mathrm{T} = 400$ K is smaller than that at $\mathrm{T} = 200$ K for both $\mathrm{V_{bg}} = -1$ V and $\mathrm{V_{bg}} = 1$ V. However, as T increases from 200 K to 400 K, the impact of carrier centroid reduces $\Delta \psi_s^{\mathrm{QM}}$ for $\mathrm{V_{bg}} = -1$ V, while the impact of carrier centroid increases $\Delta \psi_s^{\mathrm{QM}}$ and compensates the impact from $(E_0 - E_{C,\min})$. This explains Fig. 13(a). In other words, the dominance of electrical confinement increases with decreasing $\mathrm{V_{bg}}$, resulting in the QC-reduced $\mathrm{V_{bg}}$-dependence of $|\Delta \mathrm{V_{th}}/\Delta \mathrm{T}|$ for the UTB GeOI and InGaAs-OI devices in Fig. 12.

V. Conclusion

We have investigated the impact of backgate bias on the $\mathrm{V_{th}}$ sensitivity to process and temperature variations for GeOI

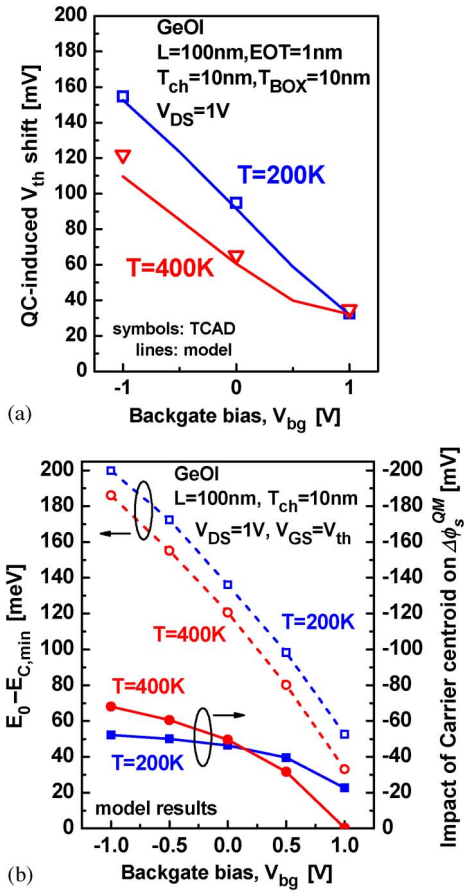

Fig. 13. (a) The difference of QC-induced V_{th} shift between T = 200 K and T = 400 K for the UTB GeOI device with various V_{bg}. (b) The ground-state eigenenergy and the impact of carrier centroid on $\Delta\psi_s^{QM}$ of the UTB GeOI device with various V_{bg} at T = 200 K and T = 400 K.

and InGaAs-OI devices. Our study indicates that the QC effect reduces the sensitivity of the L-induced V_{th} variation to V_{bg}. In other words, the V_{bg} dependence of the within-die V_{th} variation will be suppressed by the QC effect as the adaptive body bias technique [16]–[18] is utilized to compensate the die-to-die variation. This beneficial effect simplifies the design of ABB circuitry. In addition, the V_{bg} dependence of the V_{th} sensitivity to temperature variation is suppressed, and the V_{bg} dependence of V_{th} sensitivity to T_{ch} is reduced for these UTB hetero-channel devices. For the maximum value of V_{th} sensitivity, the worst-case $\Delta V_{th,L}$ is reduced by the QC effect at $V_{bg} = 1$ V, while the worst-case $\Delta V_{th,Tch}$ and $|\Delta V_{th}/\Delta T|$ occurring at $V_{bg} = 1$ V are hardly changed by the QC effect. Since Si, Ge, and InGaAs channels exhibit different degree of quantum confinement due to different quantization effective mass, the impact of quantum confinement has to be considered when one-to-one comparisons among the hetero-channel devices regarding variability are made. Our study is critical for the functional robustness of multi-V_{th} designs with advanced UTB technologies.

ACKNOWLEDGMENT

The authors are grateful to anonymous referees for critical reading of the manuscript and valuable feedback.

REFERENCES

[1] B. Vaidyanathan and A. S. Oates, "Technology scaling effect on the relative impact of NBTI and process variation on the reliability of digital circuits," *IEEE Trans. Device Mater. Rel.*, vol. 12, no. 2, pp. 428–436, Jun. 2012.

[2] X. Wang, A. R. Brown, B. Cheng, and A. Asenov, "Statistical variability and reliability in nanoscale FinFETs," in *IEDM Tech. Dig.*, 2011, pp. 5.4.1–5.4.4.

[3] E. Amat, C. G. Almudever, N. Aymerich, R. Canal, and A. Rubio, "Variability mitigation mechanisms in scaled 3T1D-DRAM memories to 22 nm and beyond," *IEEE Trans. Device Mater. Rel.*, vol. 13, no. 1, pp. 103–109, Mar. 2013.

[4] J.-S. Yuan and S. Chen, "A simulation study of Colpitts oscillator reliability and variability," *IEEE Trans. Device Mater. Rel.*, vol. 12, no. 3, pp. 576–581, Sep. 2012.

[5] V. P.-H. Hu, M.-L. Fan, P. Su, and C.-T. Chuang, "Analysis of ultra-thin-body SOI subthreshold SRAM considering line-edge roughness, work function variation, and temperature sensitivity," *IEEE J. Emerg. Sel. Topics Circuits Syst.*, vol. 1, no. 3, pp. 335–342, Sep. 2011.

[6] [Online]. Available: http://www.itrs.net/

[7] M. Radosavljevic, B. Chu-Kung, S. Corcoran, G. Dewey, M. K. Hudait, J. M. Fastenau, J. Kavalieros, W. K. Liu, D. Lubyshev, M. Metz, K. Millard, N. Mukherjee, W. Rachmady, U. Shah, and R. Chau, "Advanced high-K gate dielectric for high-performance short-channel $In_{0.7}Ga_{0.3}As$ quantum well field effect transistors on silicon substrate for low power logic applications," in *IEDM Tech. Dig.*, 2009, pp. 1–4.

[8] S. H. Kim, M. Yokoyama, N. Taoka, R. Nakane, T. Yasuda, O. Ichikawa, N. Fukuhara, M. Hata, M. Takenaka, and S. Takagi, "Sub-60 nm deeply-scaled channel length extremely-thin body $In_xGa_{1-x}As$-on-insulator MOSFETs on Si with Ni–InGaAs metal S/D and MOS interface buffer engineering," in *VLSI Symp. Tech. Dig.*, Jun. 2012, pp. 177–178.

[9] E. Pop, C. O. Chui, S. Sinha, R. Dutton, and K. Goodson, "Electro-thermal comparison and performance optimization of thin-body SOI and GOI MOSFETs," in *IEDM Tech. Dig.*, 2004, pp. 411–414.

[10] S. W. Bedell, A. Majumdar, J. A. Ott, J. Arnold, K. Fogel, S. J. Koester, and D. K. Sadana, "Mobility scaling in short-channel length strained Ge-on-insulator P-MOSFETs," *IEEE Electron Device Lett.*, vol. 29, no. 7, pp. 811–813, Jul. 2008.

[11] F. Andrieu, O. Weber, J. Mazurier, O. Thomas, J.-P. Noel, C. Fenouillet-Beranger, J.-P. Mazellier, P. Perreau, T. Poiroux, Y. Morand, T. Morel, S. Allegret, V. Loup, S. Barnola, F. Martin, J. F. Damlencourt, I. Servin, M. Casse, X. Garros, O. Rozeau, M.-A. Jaud, G. Cibrario, J. Cluzel, A. Toffoli, F. Allain, R. Kies, D. Lafond, V. Delaye, C. Tabone, L. Tosti, L. Brevard, P. Gaud, V. Paruchuri, K. K. Bourdelle, W. Schwarzenbach, O. Bonnin, B. Y. Nguyen, B. Doris, F. Buf, T. Skotnicki, and O. Faynot, "Low leakage and low variability ultra-thin body and buried oxide (UT2B) SOI technology for 20 nm low power CMOS and beyond," in *VLSI Symp. Tech. Dig.*, Jun. 2010, pp. 57–58.

[12] C. Fenouillet-Béranger, O. Thomas, P. Perreau, J.-P. Noel, A. Bajolet, S. Haendler, L. Tosti, S. Barnola, R. Beneyton, C. Perrot, C. de Buttet, F. Abbate, F. Baron, B. Pernet, Y. Campidelli, L. Pinzelli, P. Gouraud, M. Casse, C. Borowiak, O. Weber, F. Andrieu, S. Denorme, F. Boeuf, O. Faynot, T. Skotnicki, K. K. Bourdelle, B. Y. Nguyen, and F. Boedt, "Efficient multi-VT FDSOI technology with UTBOX for low power circuit design," in *VLSI Symp. Tech. Dig.*, Jun. 2010, pp. 65–66.

[13] Q. Liu, A. Yagishita, N. Loubet, A. Khakifirooz, P. Kulkarni, T. Yamamoto, K. Cheng, M. Fujiwara, J. Cai, D. Dorman, S. Mehta, P. Khare, K. Yako, Y. Zhu, S. Mignot, S. Kanakasabapathy, S. Monfray, F. Boeuf, C. Koburger, H. Sunamura, S. Ponoth, A. Reznicek, B. Haran, A. Upham, R. Johnson, L. F. Edge, J. Kuss, T. Levin, N. Berliner, E. Leobandung, T. Skotnicki, M. Hane, H. Bu, K. Ishimaru, W. Kleemeier, M. Takayanagi, B. Doris, and R. Sampson, "Ultra-thin-body and BOX (UTBB) fully depleted (FD) device integration for 22 nm node and beyond," in *VLSI Symp. Tech. Dig.*, Jun. 2010, pp. 61–62.

[14] O. Weber, O. Faynot, F. Andrieu, C. Buj-Dufournet, F. Allain, P. Scheiblin, J. Foucher, N. Daval, D. Lafond, L. Tosti, L. Brevard, O. Rozeau, C. Fenouillet-Beranger, M. Marin, F. Boeuf, D. Delprat, K. Bourdelle, B. Y. Nguyen, and S. Deleonibus, "High immunity to threshold voltage variability in undoped ultra-thin FDSOI MOSFETs and its physical understanding," in *IEDM Tech. Dig.*, Dec. 2008, pp. 1–4.

[15] K. Cheng, A. Khakifirooz, P. Kulkarni, S. Kanakasabapathy, S. Schmitz, A. Reznicek, T. Adam, Y. Zhu, J. Li, J. Faltermeier, T. Furukawa, L. F. Edge, B. Haran, S.-C. Seo, P. Jamison, J. Holt, X. Li, R. Loesing, Z. Zhu, R. Johnson, A. Upham, T. Levin, M. Smalley, J. Herman, M. Di, J. Wang, D. Sadana, P. Kozlowski, H. Bu, B. Doris, and

J. O'Neill, "Fully depleted extremely thin SOI technology fabricated by a novel integration scheme featuring implant-free, zero-silicon-loss, and faceted raised source/drain," in *VLSI Symp. Tech. Dig.*, Jun. 2009, pp. 212–213.
[16] J. W. Tschanz, J. T. Kao, S. G. Narendra, R. Nair, D. A. Antoniadis, A. P. Chandrakasan, and V. De, "Adaptive body bias for reducing impacts of die-to-die and within-die parameter variation on microprocessor frequency and leakage," *IEEE J. Solid-State Circuits*, vol. 37, no. 11, pp. 1396–1402, Nov. 2002.
[17] S. Narendra, D. Antoniadis, and V. De, "Impact of using adaptive body bias to die-to-die Vt variation on within-die Vt variation," in *Proc. ISLPED*, Aug. 1999, pp. 229–232.
[18] Y. Yasuda, Y. Akiyama, Y. Yamagata, Y. Goto, and K. Imai, "Design methodology of body-biasing scheme for low power system LSI with multi-V_{th} transistors," *IEEE Trans. Electron Devices*, vol. 54, no. 11, pp. 2946–2952, Nov. 2007.
[19] H. Mostafa, M. Anis, and M. Elmasry, "Adaptive body bias for reducing the impacts of NBTI and process variations on 6T SRAM cells," *IEEE Trans. Circuits Syst. I, Reg. Papers*, vol. 58, no. 12, pp. 2859–2871, Dec. 2011.
[20] V. P. Trivedi and J. G. Fossum, "Quantum–mechanical effects on the threshold voltage of undoped double-gate MOSFETs," *IEEE Electron Device Lett.*, vol. 26, no. 8, pp. 579–582, Aug. 2005.
[21] C.-H. Yu, Y.-S. Wu, V. P.-H. Hu, and P. Su, "Impact of quantum confinement on subthreshold swing and electrostatic integrity of ultra-thin-body GeOI and InGaAs-OI n-MOSFETs," *IEEE Trans. Nanotechnol.*, vol. 11, no. 2, pp. 287–291, Mar. 2012.
[22] V. P.-H. Hu, Y.-S. Wu, and P. Su, "Investigation of electrostatic integrity for ultrathin-body Germanium-on-nothing MOSFET," *IEEE Trans. Nanotechnol.*, vol. 10, no. 2, pp. 325–330, Mar. 2011.
[23] F. Stern and W. E. Howard, "Properties of semiconductor surface inversion layers in the electric quantum limit," *Phys. Rev.*, vol. 163, no. 3, pp. 816–835, Nov. 1967.
[24] K. H. Goetz, D. Bimberg, H. Jurgensen, J. Selders, A. V. Solomonov, G. F. Glinskii, and M. Razeghi, "Optical and crystallographic properties and impurity incorporation $Ga_xIn_{1-x}As$ $(0.44 < x < 0.49)$ grown by liquid phase epitaxy, vapor phase epitaxy, and metal organic chemical vapor deposition," *J. Appl. Phys.*, vol. 54, no. 8, pp. 4543–4552, Aug. 1983.
[25] H. Ananthan and K. Roy, "A compact physical model for yield under gate length and body thickness variations in nanoscale double-gate CMOS," *IEEE Trans. Electron Devices*, vol. 53, no. 9, pp. 2151–2159, Sep. 2006.
[26] Y.-S. Wu and P. Su, "Sensitivity of gate-all-around nanowire MOSFETs to process variation—A comparison with multigate MOSFETs," *IEEE Trans. Electron Devices*, vol. 55, no. 11, pp. 3042–3047, Nov. 2008.
[27] X. Liang and Y. Taur, "A 2-D analytical solution for SCEs in DG MOSFETs," *IEEE Trans. Electron Devices*, vol. 51, no. 9, pp. 1385–1391, Sep. 2004.
[28] *ATLAS User's Manual*, SILVACO, Santa Clara, CA, USA, 2008.
[29] Y. Taur and T. H. Ning, *Fundamentals of Modern VLSI Devices*. Cambridge, U.K.: Cambridge Univ. Press, 1998, p. 198.
[30] M. J. van Dort, P. H. Woerlee, A. J. Walker, C. A. H. Juffermans, and H. Lifka, "Quantum–mechanical threshold voltage shifts of MOSFETs caused by high levels of channel doping," in *IEDM Tech. Dig.*, Dec. 1991, pp. 495–498.
[31] O. Faynot, F. Andrieu, O. Weber, C. Fenouillet-Beranger, P. Perreau, J. Mazurier, T. Benoist, O. Rozeau, T. Poiroux, M. Vinet, L. Grenouillet, J.-P. Noel, N. Posseme, S. Barnola, F. Martin, C. Lapeyre, M. Casse, X. Garros, M.-A. Jaud, O. Thomas, G. Cibrario, L. Tosti, L. Brevard, C. Tabone, P. Gaud, S. Barraud, T. Ernst, and S. Deleonibus, "Planar fully depleted SOI technology: A powerful architecture for the 20nm node and beyond," in *IEDM Tech. Dig.*, 2010, pp. 3.2.1–3.2.4.
[32] S. M. Sze and K. K. Ng, *Physics of Semiconductor Devices*. Hoboken, NJ, USA: Wiley, 2007, p. 789.
[33] Y. A. Goldberg and N. M. Schmidt, *Handbook Series on Semiconductor Parameters*, M. Levinshtein, S. Rumyantsev, and M. Shur, Eds. London, U.K.: World Scientific, 1999, pp. 62–88.

Chang-Hung Yu (S'11) received the B.S. degree in 2007 from the National Taiwan University, Taipei, Taiwan, and the M.S. degree in 2011 from the National Chiao Tung University, Hsinchu, Taiwan, where he is currently working toward the Ph.D. degree at the Institute of Electronics.

His current research interests include design and modeling of emerging CMOS devices.

Pin Su (S'98–M'02) received the B.S. and M.S. degrees in electronics engineering from National Chiao Tung University, Hsinchu, Taiwan, and the Ph.D. degree from the Department of Electrical Engineering and Computer Sciences, University of California at Berkeley, Berkeley, CA, USA.

From 1997 to 2003, he conducted his doctoral and postdoctoral research in silicon-on-insulator (SOI) devices in Berkeley. He was also one of the major contributors to the unified BSIMSOI model, the first industrial standard SOI MOSFET model for circuit design. Since August 2003, he has been with the Department of Electronics Engineering, National Chiao Tung University, where he is currently a Professor. He has authored or coauthored over 160 research papers regarding his research interests in refereed journals and international conference proceedings. His research interests include silicon-based nanoelectronics, modeling and design for exploratory CMOS devices for ultralow-power applications, and circuit–device interaction and co-optimization in nanoscale CMOS.

Prof. Su serves in the technical committee of the IEEE International Electron Devices Meeting.